Atmos. Chem. Phys. Discuss., 11, 11739–11769, 2011
www.atmos-chem-phys-discuss.net/11/11739/2011/
doi:10.5194/acpd-11-11739-2011

Atmospheric Chemistry and Physics Discussions

The breakup of levitating water drops observed with a high speed camera

C. Emersic and P. J. Connolly

School of Earth, Atmospheric and Environmental Sciences, The University of Manchester, Manchester, UK

Received: 6 April 2011 – Accepted: 7 April 2011 – Published: 15 April 2011

Correspondence to: C. Emersic (christopher.emersic@manchester.ac.uk)

Published by Copernicus Publications on behalf of the European Geosciences Union.

Abstract

A wind tunnel was used to interact water drops and were recorded using a high speed camera. Three distinct collisional breakup types were observed and the drop size spectra from each were analysed for comparison with parameterisations constructed by Low and List (1982a). The spectra predicted by the parameterisations did not accurately correlate with the observed breakup distributions for each breakup type when applied to the relatively larger and similarly-sized drop-pairs of size 4–8 mm, comparable to those sometimes observed in nature. We discuss possible reasons for the discrepancies and suggest potential areas for future investigation. A computer programme was subsequently used to solve the stochastic coalescence and breakup equation using the Low and List breakup parameterisation, and the evolving drop spectra for a range of initial conditions were examined. Initial cloud liquid water content was found to be the most influential parameter, whereas initial drop number was found to have relatively little influence. This may have implications when considering the effect of aerosol on cloud evolution, raindrop formation and resulting drop spectra.

1 Introduction

Raindrop breakup events are important to the evolution and formation of drop spectra in precipitating clouds, particularly for warm rain processes in which frequent collision, coalescence and breakup events play a major role in the production of raindrop-sized precipitation. McFarquhar (2004a) found from modelling studies that the variation in raindrop size distributions depends heavily on the drop distribution at precipitation onset, and that the large spread in the breakup distributions can account for the inability of equilibrium distributions to form in nature. Clustering of raindrops was also found to increase the chances of interactions between drop-pairs, as larger drops overtake smaller ones during descent. However, McFarquhar (2004b) recognised that the certainty with which the collision-induced breakup of raindrops can be predicted is limited.

ACPD
11, 11739–11769, 2011

The spontaneous – or aerodynamic – breakup of larger drops may have some significance to drop spectrum evolution, for instance when large raindrops are produced from melting snow. In general however, spontaneous drop breakup is not considered to be as influential to the resulting raindrop size distribution in warm rain processes owing to difficulties in large drops forming without prior collisionally-induced breakup occurring (Magarvey and Geldart, 1962; Low and List, 1982b). Nevertheless, Hobbs and Rangno (2004) conducted airborne measurements beneath cumulus congestus clouds formed in one case by a biomass fire in Brazil, and in another case, in very clean but atmospherically unstable conditions in the Marshall Islands in the tropical Pacific Ocean, and observed very large raindrops in their associated rainshafts of the order of 1 cm in diameter. These drops were thought to have formed rapidly by the coalescence of drops in narrow regions of the cloud where liquid water contents were unusually high. It is also suspected that large drops can form in the regions between updraughts where drop-drop collisions (and therefore breakups) are minimised but that scavenging of smaller cloud droplets can lead to drop growth to ∼8 mm as observed by Beard et al. (1986). Studies of spontaneous breakup of larger drops have also been conducted (Villermaux and Bossa, 2009) and have shown that drop spectra similar to those observed in nature can be produced.

Modelling studies examining how the drop spectra in rain producing clouds evolve over time have found that three-peaked distributions can form (Mcfarquhar and List, 1991a, b; List and Mcfarquhar, 1990). In their 1-D simulations, multiple pulses of rain with durations of between 2–10 min at a repeated rate of every 4–12 min at the top of the shaft led to drops arriving in packages at the ground, with the largest drops arriving first in each package. Averaged over time, the three-peak distributions were observed. Simulations in which overlapping was prevented did not produce the three-peak spectra, and it was proposed that the drop interactions from their differing terminal velocities were necessary for subsequent coalescence and breakup events to give rise to the distribution peaks. A number of observations have measured multiple drop distribution peaks at similar sizes to those modelled (Debeauville et al., 1988;

ACPD
11, 11739–11769, 2011

The breakup of levitating water drops

C. Emersic and P. J. Connolly

Steiner and Waldvogel, 1987; Willis, 1984; Zawadzki and Antonio, 1988); however, some observational studies have noted spectra without multiple modes or with time- and altitude-varying single modes (Joss and Gori, 1978; Warner, 1969).

Limited laboratory investigations have examined collisional drop breakup processes, and the few studies conducted to date (e.g. Barros et al., 2008; Low and List, 1982b; Mctaggart-Cowan and List, 1975) have noted discrepancies in the drop concentrations and modal sizes for given breakup types that have been attributed to experimental differences. This investigation examines the size distributions of water drop breakup events using recently available high speed video technology. Drops levitated in an air stream were recorded breaking up after collisions with other drops. Breakup events were categorised into three distinct types: filament, sheet, and bag (sometimes referred to as disc) (defined in Sect. 3.1), with the resulting fragment distributions for each being compared to those parameterised by Low and List (1982a) through the use of a computer programme.

A description of the experimental procedure is presented in Sect. 2, experimental observations and the results of computer simulations are presented in Sect. 3, and a discussion of findings is presented in Sect. 4. A summary is given in Sect. 5.

2 Experimental setup and procedure

Experiments were conducted using a vertical wind tunnel (Fig. 1). Air is passed through a settling chamber before passing out through an upper orifice, and a wire grate covers the orifice which produces a radial velocity profile from the centre where the air speed is lowest. The presence of an upper plate provides a back-pressure, which combined with the radial velocity profile, generates a stagnation pressure well in which injected drops can levitate. Additional drops can then be injected into the air stream which find their way into the well and may interact with any drop present. The airspeed as a function of radius in the well in the general region where the drops oscillate was measured using a calibrated hot wire probe to be $10.4 \pm 0.5\,\mathrm{m\,s^{-1}}$ in the centre, with

Discussion Paper | Discussion Paper | Discussion Paper | Discussion Paper |

ACPD

11, 11739–11769, 2011

The breakup of levitating water drops

C. Emersic and P. J. Connolly

an edge speed of $12.6 \pm 0.5\,\mathrm{m\,s^{-1}}$; the theoretical terminal velocity of drops of the size used here is $\sim 9\,\mathrm{m\,s^{-1}}$ (Pruppacher and Klett, 1978, Fig. 10–25, 420 pp.). The airspeed in the pressure well decreases with height and so drops oscillating within it will fluctuate in height about the position where the airstream is equal to their terminal velocity.

Levitated drops were filmed using a high-speed camera (Photron Fastcam MC-1) at 2000 frames per second which allowed breakup drops to be resolved to a minimum of 1 mm diameter. The spatial resolution available could not be improved accurately beyond 1 mm, without reducing the field-of-view, and thus an analysis of fine-scale, sum-mm drop breakup structure was not possible; it was however not necessary for this study.

Water drops were injected from above and fell into the well. Precise control over drop size was not possible; however, the drop impacting from above was always smaller than the levitated drop and measured from the video (Table 1). This is in contrast to nature where larger drops with a greater terminal velocity are more likely to impact from above onto a smaller drop. The larger levitating drop was approximately stationary during the brief collision event and therefore at its terminal velocity. This experimental setup was dissimilar to that employed by Barros et al. (2008) and Low and List (1982b) who had greater control over drop size, where both drops were nearer terminal velocity at collision given greater fall heights, and where larger, faster falling drops fell from above onto smaller drops. Nevertheless we felt this approach was appropriate to address the aims of this study.

A total of 25 collisional drop breakup events were examined here. Resulting breakup drops were counted by hand, post video analysis, and binned to 1 mm size; resolution limitations prevented higher accuracy. Note thus, that all particles 1 mm or smaller were binned as 1 mm.

3 Results

3.1 Experimental observations and simulated breakup distribution comparisons

As found by other researchers, colliding drop-pairs were observed to breakup in three distinct ways: as filament, sheet, or bag (Fig. 2). Of the 25 drop-breakup events observed here, 8 were filaments, 4 were sheets, and 13 were bags. For filament breakup, after collision, the drops briefly coalesce and then separate. The original drop sizes are often restored and an interconnecting bridge between them forms before disintegrating into a spectrum of smaller drops (Fig. 2i). The disintegration of the filament bridge tends to depend on the thickness variations along its length; the thicker parts typically form larger drops as the filament destabilises and pinches during drop formation. For sheets, the resulting coalesced drop tends to flatten out roughly horizontally before lifting at one edge and disintegrating into many smaller drops (Fig. 2ii). Bag breakups are similar to sheets initially; after the resulting coalescencedrop flattens out, its centre lifts and arches in the air stream to form a thinning bag, edged by the drop rim containing the bulk water (Fig. 2iii). This bag rapidly expands before bursting explosively to produce numerous smaller drops. The size of the bag and its inflation depth varied widely and were likely related to the thickness of the initially arching drop centre.

The resulting drop sizes, estimated impact velocity, and breakup type are summarised in Table 1, and the resulting drop spectra are shown in Fig. 3. The impact speed of the colliding smaller drop was comparable in all successful breakup events of any breakup type, between ∼0.3–0.7 $\mathrm{m\,s^{-1}}$ with a standard deviation of 0.13 (Table 1), which is comparable to drop impact velocities of this size in natural clouds (Pruppacher and Klett, 1978, Fig. 10–25, 420 pp.). The theoretical relative difference in terminal velocity between drop-pairs of the sizes used here is also shown in Table 1 and is comparable to those observed. Fragment distributions were also computed using the parameterisations given by Low and List (1982a) for comparison (details of this

ACPD
11, 11739–11769, 2011

computation are given in Appendix A). These were then plotted against those experimentally observed in Fig. 3.

The observed breakup distributions (Fig. 3), pink lines) reveal a consistent pattern of increasing drop concentration with decreasing drop size for a given breakup type. The concentration of smaller drops (1 mm or less in diameter) increases as breakup type transitions from filament (~40% of total, Fig. 3i), through sheet (~50%, Fig. 3ii), to bag breakup (~75%, Fig. 3iii), where explosive breakup was more likely to be observed. Sheet and bag breakup produced relatively fewer larger drops (1 mm or larger) than filament breakup, as would be expected from a greater portion of the coalesced drop mass transferring to predominantly larger concentrations of smaller drops on breakup for those two breakup types. Sheet breakup had slightly higher concentrations of drops 2–3 mm in diameter than bag breakup, consistent with the reduced breakup explosiveness. The interquartile range in the observed distributions was greatest for smaller drop sizes for all breakup types; the number of small drops produced was highly variable to the particular breakup event. Larger drops were more consistent in concentration with the exception of filament breakup, whose propensity to produce larger drops more frequently led to greater variability between breakup events.

The computed distributions using the Low and List parameterisations (Fig. 3, blue lines) for the sizes of drop-pairs used here show a greater normalised concentration of drops for resulting drop sizes greater than 1 mm relative to those observed; however, this was not true for drops 1 mm or less, where normalised concentrations were substantially less than observed – which is unexpected given our relative insensitivity to these smaller sizes due to resolution restrictions. The predicted distributions also consistently reveal a mode at the largest drop size for all breakup types. For filament breakup, the predicted distribution shows a fairly consistent concentration, without an apparent gap, between the smallest and largest drop sizes, but the observed distributions reveal a more pronounced saddle between these modes.

In addition to standard coalescence and breakup events listed in Table 1, we observed separately an instance where a potential filament breakup event failed and

ACPD
11, 11739–11769, 2011

C. Emersic and P. J. Connolly

the drop did not breakup, but re-coalesced into a flattened drop before entering bag breakup within a few hundred milliseconds. We also observed two instances of breakup occurring twice in succession (<1 s): the first involved a filament breakup followed by a bag breakup of the larger remaining drop; the second involved two bag breakups where after the first breakup, a large enough drop remained to break up again as a secondary bag breakup event. This type of double breakup is not currently modelled when applying the Low and List breakup parameterisation to the stochastic coalescence and breakup equation; however, it is difficult to judge the statistical relevance of this type of event.

3.2 Simulation of stochastic coalescence and breakup

The evolution through coalescence and breakup of an initial drop spectrum was simulated through the solution of the stochastic coalescence and breakup equation. Details of these computations are given in Appendix B. Cloud spectra evolution was simulated for 1500 s with the spontaneous breakup scheme active in all cases to examine how drop mass-weighted mean diameter (Fig. 4a) and concentration (Fig. 4b) altered. Initial cloud drop concentration and cloud liquid water content were varied for cases when collisional breakup was active and inactive to test sensitivity. The resulting drop size distributions are shown in Fig. 5.

Figure 4 reveals that the time to reach a steady-state in mean drop size and concentration is heavily influenced by the cloud liquid water content, with greater values allowing steady-state to be reached earlier; a value of 3×10^{-3} kg kg^{-1} allows steady-state to be reached by ~500 s, and 1×10^{-3} kg kg^{-1} by ~1500 s. Collisional breakup reduces the resulting steady-state mean drop diameter from ~2.5 mm to ~0.5 mm, which is not significantly changed by initial cloud liquid water content. Similarly, steady-state drop concentration was increased by collisional breakup from $\sim 1.5 \times 10^3$ m^{-3} to $\sim 7 \times 10^4$ m^{-3}. The initial drop concentration had less effect on the time taken to reach steady-state; a factor of 5 increase in initial drop concentration led to a delay of ~100 s to reach steady-state. The initial drop concentration had no effect on the resulting

ACPD
11, 11739–11769, 2011

C. Emersic and P. J. Connolly

mean size or resulting drop concentration; however, its effect on the rate of change of spectrum evolution was slight, with increasing initial drop concentrations resulting in more rapid mean size and concentration changes as steady-state is approached – this follows from the reduced initial concentration that increasing initial drop number causes for a fixed initial cloud liquid water content.

The resulting drop spectra (Fig. 5) show no presence of a three-peaked distribution. Increasing initial cloud liquid water content increases the maximum drop size by 0.5 mm to ~3 mm when collisional breakup is active. In the absence of collisional breakup, the resulting distribution is markedly broadened, particularly for greater initial cloud liquid water contents. The initial drop concentration has negligible effect on the resulting distribution regardless of whether or not collisional breakup is active.

The computations highlight the substantial influence that collisional breakup has on the resulting spectra. The number of larger drops (>3 mm) that result is small according to the Low and List parameterisations (Fig. 5); however drops much larger than this have been observed in nature at high liquid water contents (Hobbs and Rangno, 2004). Figure 6 shows both the time varying percentage fraction of total collisions, and percentage fraction of total fragments that the Low and List parameterisations predict should occur from drops of size 4 and 6 mm (comparable in size with the mean sizes used in the experiments here (Table 1) for two high values of cloud liquid water content of 3 and 5 $\mathrm{kg\,kg^{-1}}$. It is assumed that a precipitating drop concentration of $1\times10^{-3}\,\mathrm{l^{-1}}$ is present initially in the rain shaft, with an exponential drop size distribution. Spontaneous breakup is not represented in the calculations to ensure only the collisionally-induced contributions to breakup events are represented to be consistent with the experimental observations. The Low and List parameterisations suggest that a maximum of ~0.2–0.4% of total breakup events are expected to be contributed by the larger 4 and 6 mm drop-pair interactions and ~0.5–1.1% of all breakup fragments. These fractions reduce in value rapidly and are negligible by 100 s. It is possible to compare the prediction of percentage fragment contributions with an equivalent result based on the experimental observations. By comparing the number of observed

ACPD
11, 11739–11769, 2011

experimental breakup fragments with those estimated from the distributions resulting from the Low and List parameterisations, it is possible to find adjustment factors for each breakup type to apply to Fig. 6, to quantify the underestimation of fragment concentrations of the Low and List parameterisations for the drop-pair sizes used in the observations. Appendix C describes the method to establish the estimated parameterised fragment concentrations used to determine these factors, and these are listed in Table 2. The estimated number of fragments that the Low and List parameterisations predict after 4 and 6 mm drops interact is very low; in the case of bag breakup, the result appears to be non-physical, with less than the two initial colliding drops resulting. Relative to the values observed experimentally, there is a factor of ~4 fewer total fragments predicted for filament and sheet breakup, and a factor of ~42 fewer for bag breakup. After adjustment of the maximum percentage contributing fractions in Fig. 6, as many as ~2–5% of total fragment drops could actually be contributed by the larger drop-pair interactions for filament and sheet breakup, and a substantial ~20–45% by bag breakup.

4 Discussion

A wind tunnel was used to levitate water drops such that additional drops could impact and induce collisional breakup. The resulting drop spectra were observed from breakup events for each of three categories of breakup: filament, sheet and bag. These distributions were compared to those predicted by a computer programme using parameterisations given by Low and List (1982a). Subsequently, a second computer programme was used to examine cloud evolution and final spectra after stochastic drop breakup events occurred.

ACPD
11, 11739–11769, 2011

4.1 Observed and predicted drop spectra comparison

The observed breakup distributions (Fig. 3) revealed increasing numbers of smaller drops (1 mm or less) as breakup type transitioned from filament (~40% of total), through sheet (~50%), to bag breakup (~75%). This trend is qualitatively consistent with the experimental observations of other researchers (e.g. Barros et al., 2008) whose used an alternative experimental setup where their drop-pairs were falling at true terminal velocity prior to collision, in contrast to here where the larger drop was levitated and the smaller drop fell from above at approximately its terminal velocity (Table 1).

There are two noteworthy general discrepancies between the applied parameterisations of Low and List (1982a) and our observed results (Fig. 3):

1. The parameterisations predict greater normalised concentrations of drops 2 mm or larger than were observed for all breakup types for the drop size combination occurring in our experiments.

2. We observed greater normalised concentrations of smaller drops (1 mm or less) in all breakup types than suggested by the Low and List parameterisations – a factor of ~4 for filament and sheet breakup, and ~8 for bag breakup. This discrepancy occurs despite our relative lack of sensitivity to very small particles due to spatial resolution limitations.

It is possible that these discrepancies result from the Low and List parameterisations being less applicable to the drop-pair sizes used in these experiments; those used by Low and List (1982b) had size ratios between 1.8–11.4, in comparison to the 1.0–2.0 ratios here (Table 1). In general, the parameterisations of Low and List may only have application to the drop-pair sizes used in the experiments from which they were constructed (larger size ratios are, however, likely to be more representative of breakup events inside natural clouds, Mcfarquhar and List, 1991b). This is further supported by two further notable differences in the filament breakup distributions in Fig. 3iii: (a) the

ACPD
11, 11739–11769, 2011

presence of a saddle between the two observed distribution modes; (b) the observed shifting to a smaller size of the mode corresponding to the larger original drops. The saddle, (a), is possibly a consequence of how the filament bridge forms between drop-pairs of a given size; in the case observed here with two larger drops 4–6 mm in diameter, the bridge that formed was often substantial, containing a greater water mass. This often allowed greater filament length before beading, and thus led to greater numbers of smaller drops, to form a more substantial mode at smaller sizes (Fig. 3iii). A shorter bridge would more likely be formed by smaller parent drops, and result in less beading to result in drop sizes more comparable to the parent drop sizes, and distributions more comparable to those described by the Low and List parameterisations. Furthermore, because the drops used here where larger than have been used previously, it is more likely that they will be separated in size in the resulting distribution from the smaller fragments of the bridge. The modal size shift, (b), is likely a consequence of mass conservation; the second mode at larger size (Fig. 3iii) corresponds to a size slightly smaller than the parent drop sizes. In filament breakup, the parent drops are typically restored, with mass lost to form the filament bridge; the corresponding reduction in drop size is represented by this second mode. No such correspondence between secondary mode and parent drop size is observed by the Low and List parameterisations; the second mode remains centred on the larger drop size after breakup. This may suggest that conservation of mass requires a more complete treatment in breakup parameterisations.

Our observed distributions for the drop-pair sizes interacted here may be more representative of nature than those predicted, particularly for sheet and bag breakup, given the considerably greater concentrations of smaller drops observed. The impact velocity of the colliding drops was comparable in all observed breakup events (Table 1) and with colliding drops in natural clouds (Pruppacher and Klett, 1978), yet we observed the full range of breakup types: filament, sheet and bag. This is possibly in contrast to the observations of Low and List (1982b) who found that a kinetic energy dependence governed the probability of drop breakup type. However, only 25 breakup events

ACPD
11, 11739–11769, 2011

were observed here, which constitutes a considerably smaller sample size than used by other researchers. Furthermore, unsuccessful breakup events were not recorded and thus determining the probability of a particular breakup type was not possible. Once a given breakup type had initiated and the drop was shaped appropriately and accelerating, the resulting drop distributions between similar breakup events seemed determined to a greater degree by the fine-scale shape of the drop, which was highly variable despite similar impact velocities and drop-pair sizes.

We also noticed, separately from the data presented, two instances of multibreakup events following a collision between drops. In the first, a filament breakup was followed by a bag breakup produced by a larger remaining drop; in the second, a bag breakup produced a larger drop from the re-coalescence of the bag rim which itself then experienced a subsequent bag breakup a few ms later. Multiple breakup events such as these are undocumented in the literature to our knowledge and could affect the resulting drop distributions. They are also not accounted for by current parameterisations and are not currently modelled when applying the Low and List breakup parameterisation to the stochastic coalescence and breakup equation. Their apparent relative infrequency may not produce a significant overall influence in natural raindrop spectrum evolution; however, further investigations into the probability of such multiple-breakup events occurring may be beneficial.

4.2 Drop spectrum evolution

A computer programme was used to solve the stochastic coalescence and breakup equation (Sect. 3.2) to examine the evolution of an initial drop distribution. Initial drop concentration and cloud liquid water content could be varied, and cases where collisional breakup was active or inactive were examined. Spontaneous breakup of drops was simulated in all runs except where specified.

The simulations revealed that the time to reach a steady-state in mean drop size and concentration was dependent mostly on the cloud liquid water content, with greater values allowing steady-state to be reached earlier (Fig. 4). Collisional breakup reduced the resulting steady-state mean drop diameter by a factor of ∼5, which was not significantly changed by initial cloud liquid water content. Similarly, steady-state drop concentration was increased by collisional breakup by a factor of ∼50. The resulting drop spectra (Fig. 5) did not show a three-peaked distribution as observed in modelling studies by List and McFarquhar (1990) and McFarquhar and List (1991a, b) in which a requirement for such distributions appeared to be the presence of overlapping and interacting falling rain pulses.

Initial drop concentration was shown to be considerably less influential than initial liquid water content on the drop spectrum evolution; the initial drop concentration had only a relatively slight effect on the time taken to reach steady-state or on the resulting mean size or drop concentration. Its influence on the rate of change of spectrum evolution was small, with increasing initial drop concentrations resulting in slightly more rapid mean size and concentration changes as steady-state is approachedv – this follows from the reduced initial concentration that increasing initial drop number causes for a fixed initial cloud liquid water content. This rate of change is affected to a considerably greater extent from alterations in initial cloud liquid water content however. The influence of initial drop concentration also revealed to have no measureable effect on the resulting drop size distribution (Fig. 5). This may be relevant to considerations of how aerosols affect cloud microphysics (Lohmann and Feichter, 2005), and may also affect calculations of precipitation susceptibility (Ma et al., 2010; Stevens and Feingold, 2009); aerosol influences on cloud spectra, cloud evolution and rain formation may be less significant relative to parameters less dependent on aerosol such as initial cloud liquid water content (for fixed drop concentration).

The distributions observed in our experiments were considered for inclusion in the programme to solve the stochastic coalescence and breakup equation, to enable a comparison with the Low and List distributions; however, our lack of sensitivity to sizes smaller than 1 mm was considered to constitute a sufficient shortcoming for this to be possible. However, it was possible to compare the estimated distribution fragment concentration from the Low and List parameterisations with those observed. From this it

ACPD
11, 11739–11769, 2011

was possible to quantify adjustments to the predicted fraction of total breakup events from the Low and List parameterisations for drop-pairs of sizes 4 and 6 mm shown in Fig. 6 (Table 2). These larger drop sizes are observed in nature (Hobbs and Rangno, 2004), but the Low and List parameterisations were not constructed from observations of drops of such large sizes. A factor of ~4 more breakup fragments were observed than the parameterisations predicted for filament and sheet breakup types, and this increased to a factor of ~42 for bag breakup. The large factor for bag breakup is likely down to the significant number of small fragment drops observed but seemingly not accounted for by the Low and List parameterisations (Fig. 3). Applying these factors to the percentage contributing fractions of resulting fragments for 4 and 6 mm drop-pair interactions reveals that as many as ~2–5% of total fragment drops could be contributed for filament and sheet breakup, and a substantial ~20–45% by bag breakup. Experiments by Low and List (1982b), in which the likelihood of a particular breakup type was measured, found that filament breakup was the most frequently occurring type. It is therefore less likely that the high contributing fractions for bag breakup will dominate evolution in clouds containing larger drops. In determining the adjustment factors, it was noted that the number of fragments that the Low and List parameterisations predict after larger 4 and 6 mm drops interact is very low. In the case of bag breakup, the result appeared to be non-physical, with less than the two initial colliding drops resulting. This further suggests that the Low and List parameterisations may be less applicable to drop-pair sizes outside of the range used in the observations from which they were constructed.

5 Summary

A wind tunnel was used to levitate water drops while additional drops impacted from above to induce collisional breakup. Three distinct breakup types were observed using a high speed camera and the drop size spectra from each were analysed for comparison with those predicted by parameterisations constructed by Low and List (1982a).

ACPD
11, 11739–11769, 2011

An initial drop spectrum was also simulated and its evolution computed through the solution of the stochastic coalescence and breakup equation.

The experimentally observed drop spectra showed prominent differences to those predicted for our drop-pair sizes based on the Low and List parameterisations (Fig. 3). Key differences were:

1. Greater numbers of drops 2 mm or larger were predicted than observed for all breakup types.

2. Greater concentrations of drops 1 mm or smaller were observed than predicted; a factor of ∼4 more for filament and sheet breakup; a factor of ∼8 more for bag breakup. This is despite our relative insensitivity to observing sub mm drops.

3. The observed distributions, particularly for filament breakup suggest the Low and List parameterisations may not accurately account for mass conservation, and may need to be reviewed for cases where drop-pairs other than those the parameterisations were constructed for, interact, particularly larger drops of comparable size. (Further details in Sect. 4.1.)

Potential weaknesses and limitations in the experimental procedure undertaken include not interacting drops at true terminal velocity, although the difference was small (Table 1), and interacting drops of large and comparable sizes that may be less common in natural clouds; much larger drops have however been observed in natural clouds (Hobbs and Rangno, 2004). It is likely from the spectra comparisons (Fig. 3) and analysis of total fractional fragment contributions for large drops (Fig. 6, Sect. 4.2) that the observations here for the larger drop-pair sizes used are more representative than the Low and List parameterisation predictions, which were shown to under-predict fragment numbers for larger drop-pairs; the parameterisations may be less suitable for drop-pair sizes outside the observed range from which they were constructed. It is suggested that current breakup parameterisations could be addressed in future based around these findings, and we encourage further experimental studies in this area for a wider range of drop-pair sizes and larger sample sizes than available here.

ACPD
11, 11739–11769, 2011

Simulations of drop breakup (Sect. 3.2) revealed that the time for mean drop size and drop concentration steady-state to be reached was independent of whether collisional breakup was active, was loosely influenced by initial drop number, but was heavily dependent on initial cloud liquid water content (Figs. 4, 5, and Sect. 4.2). The resulting drop spectrum (Fig. 5) was again influenced heavily by initial cloud liquid water content in addition to whether collisional breakup was active. An important finding was the apparent relative lack of influence of the initial drop concentration on the resulting steady-state mean drop diameter and drop concentration, and its absence of any discernible influence on the resulting drop spectrum. This parameter only had a small influence on the rate of change of mean drop size and drop concentration at times before steady-state was reached, and the influence was substantially less significant than the equivalent effect caused by the initial cloud liquid water content (for fixed drop concentration) (Fig. 4). This may be relevant to considerations of how aerosols affect cloud microphysics.

Appendix A

Calculation of simulated fragment distributions

The parameterisation reported in Low and List (1982a), with the corrections reported in List et al. (1987), was used to calculate fragment size distributions from the collision and subsequent break up of a drop-pair. Their parameterisation calculates the fragment distribution due to breakup in 3 different breakup types: disk (bag), sheet, and filament.

For filament breakup it is assumed that two normally distributed primary modes result; one centred on the small drop diameter and the other on the large drop diameter. In addition it is assumed that a third mode results through disintegration of the adjoining bridge between the two primary drops. This mode is assumed to be log-normally distributed and the mode is parameterised to be dependent on the size of the colliding drops. For sheet breakup, two modes are assumed to result, a normally distributed mode centred on the large drop and a log-normally distributed mode that depends on the size of the smaller drop. For disk breakup there are again two modes. Firstly, a normally distributed mode – the centre of which depends on the collisional kinetic energy and surface energy – and secondly a log-normal mode that depends on the size of the smaller drop (as in sheet breakup).

For each type of breakup the relative size of each distribution is determined as described in Low and List (1982a). Once the parameters of each distribution are known they are integrated over the limits of the size bins used in this study (1 mm width) to enable fair comparison. We were not required to calculate the total breakup function (as in Low and List, 1982a) since we were able to classify each observed breakup event into the one of the three types.

The average interacting small and large drop sizes (Table 1) were used to calculate the expected breakup distributions, by integrating them between the same size bins used for our data. The total number in each bin was calculated by summing the contribution from each mode using either the difference between the cumulative normal distribution or cumulative log-normal distribution at upper and lower bin sizes.

Appendix B

Solution of the stochastic coalescence and breakup equation

Our method to solve the stochastic coalescence/breakup equation follows Bott (1998). Bott has demonstrated that this method gives excellent results when compared to the analytical solution to Golovin's kernel and when compared to the more computationally expensive Berry and Reinhart method. Also, it has been shown that a 1-moment approach is adequate for resolving stochastic breakup (Feingold et al., 1988).

A mass grid is used, of which each adjacent bin is $2^{1/2}$ times the previous bin. The number-size distribution is transformed into a mass distribution following Berry and Reinhart and the equation is integrated using a simple time-stepping scheme. Firstly

ACPD
11, 11739–11769, 2011
The breakup of levitating water drops
C. Emersic and P. J. Connolly

the loss of mass from two bins containing colliding drops is calculated using the collision kernel of Long (1974). The mass from these interacting bins is added together and the fraction that coalesces is added to the bin that is nearest to the sum of the two interacting bins – of which a fraction is then transported to the adjacent mass bin using the exponential flux method. The mass that does not coalesce is redistributed on the mass grid using the fragment distributions calculated from Low and List (1982a).

Also implemented are spontaneous breakup schemes where drops of a certain size have a finite probability of breaking up due to hydrodynamic instability, yielding a fragment distribution that is exponentially distributed (see Kamra et al., 1991; Komabayasi et al., 1964; Villermaux and Bossa, 2009).

Appendix C

Calculation of parameterisation adjustment factors

In Sect. 3.2, fragment contributions from 4 and 6 mm drop interactions relative to all interactions are predicted based on the Low and List parameterisations and solution of the stochastic coalescence and breakup equation (Appendix B). By comparing the number of observed drop fragments from the estimated number suggested by the parameterisations, factors can be established for interactions between 4 and 6 mm drops. These can then be used to adjust the fractional contribution values suggested by the parameterisations to help better indicate their overall significance to the resulting drop spectra, given that such large drops have been observed in natural clouds (Hobbs and Rangno, 2004).

ACPD
11, 11739–11769, 2011

List of terms (SI units).

M_L	Mass of large drop
M_S	Mass of small drop
M_T	Total mass
M_i	Mass of distribution element
k	Scaling factor
p_w	Density of water
P_i	Drop distribution
V_L	Volume of large drop
V_S	Volume of small drop
V_i	Volume of distribution element
D_L	Diameter of large drop
D_S	Diameter of small drop
D_i	Drop distribution fragment diameters

Considering the coalescence and breakup event, the combined masses of the two interacting drops must be equal to the mass given by the sum of the parameterised breakup distribution. This distribution is normalised and thus must have a scaling factor present to ensure it is scaled appropriately for mass, i.e. to ensure mass conservation.

$$M_L + M_S = M_T = k \sum_i M_i P_i$$

Expressing mass as a product of density and volume:

$$p_w V_L + p_w V_S = k p_w \sum_i V_i P_i$$

Water density terms cancel; volume can be expressed as a function of the diameter of a sphere:

$$\frac{\pi}{6} D_L^3 + \frac{\pi}{6} D_S^3 = \frac{\pi}{6} k \sum_i D_i^3 P_i$$

Discussion Paper | Discussion Paper | Discussion Paper | Discussion Paper |

ACPD

11, 11739–11769, 2011

Rearranging for k:

$$k = \frac{D_L^3 + D_S^3}{\sum_i D_i^3 P_i}$$

Total particle number is thus given by:

$$k \sum_i P_i$$

Acknowledgements. We would like to thank the EPSRC instrument loan pool for providing us with an opportunity to use one of their high speed cameras for this research. We would also like to thank Tom Choularton for guidance and comment during the project.

References

Barros, A. P., Prat, O. P., Shrestha, P., Testik, F. Y., and Bliven, L. F.: Revisiting Low and List (1982): Evaluation of Raindrop Collision Parameterizations Using Laboratory Observations and Modeling, J. Atmos. Sci., 65, 2983–2993, doi:10.1175/2008JAS2630.1, 2008.

Beard, K. V., Johnson, D. B., and Baumgardner, D.: Aircraft Observations of Large Raindrops in Warm, Shallow, Convective Clouds, Geophys. Res. Lett., 13, 991–994, 1986.

Bott, A.: A flux method for the numerical solution of the stochastic collection equation, J. Atmos. Sci., 55, 2284–2293, 1998.

Debeauville, C. A., Petit, R. H., and Marion, G.: Evolution of Peaks in the Spectral Distribution of Raindrops from Warm Isolated Maritime Clouds, J. Atmos. Sci., 45, 3320–3332, 1988.

Feingold, G., Tzivion, S., and Levin, Z.: Evolution of Raindrop Spectra .1. Solution to the Stochastic Collection Breakup Equation Using the Method of Moments, J. Atmos. Sci., 45, 3387–3399, 1988.

Hobbs, P. V. and Rangno, A. L.: Super-large raindrops, Geophys. Res. Lett., 31, L13102, doi:10.1029/2004gl020167, 2004.

Joss, J, and Gori, E. G.: Shapes of Raindrop Size Distributions, J. Appl. Meteorol., 17, 1054–1061, 1978.

ACPD

11, 11739–11769, 2011

The breakup of levitating water drops

C. Emersic and P. J. Connolly

Kamra, A. K., Bhalwankar, R. V., and Sathe, A. B.: Spontaneous Breakup of Charged and Uncharged Water Drops Freely Suspended in a Wind-Tunnel, J. Geophys. Res.-Atmos., 96, 17159–17168, 1991.
Komabayasi, M., Gonda, T., and Isono, K.: Life Time of Water Drops before Breaking and Size Distribution of Fragment Droplets, J. Meteor. Soc. Japan, 330–340, 1964.
List, R., Donaldson, N. R., and Stewart, R. E.: Temporal Evolution of Drop Spectra to Collisional Equilibrium in Steady and Pulsating Rain, J. Atmos. Sci., 44, 362–372, 1987.
List, R. and Mcfarquhar, G. M.: The Evolution of 3-Peak Raindrop Size Distributions in One-Dimensional Shaft Models .1. Single-Pulse Rain, J. Atmos. Sci., 47, 2996–3006, 1990.
Lohmann, U. and Feichter, J.: Global indirect aerosol effects: a review, Atmos. Chem. Phys., 5, 715–737, doi:10.5194/acp-5-715-2005, 2005.
Long, A. B.: Solutions to Droplet Collection Equation for Polynomial Kernels, J. Atmos. Sci., 31, 1040–1052, 1974.
Low, T. B. and List, R.: Collision, Coalescence and Breakup of Raindrops .2. Parameterization of Fragment Size Distributions, J. Atmos. Sci., 39, 1607–1618, 1982a.
Low, T. B. and List, R.: Collision, Coalescence and Breakup of Raindrops .1. Experimentally Established Coalescence Efficiencies and Fragment Size Distributions in Breakup, J. Atmos. Sci., 39, 1591–1606, 1982b.
Ma, X., von Salzen, K., and Cole, J.: Constraints on interactions between aerosols and clouds on a global scale from a combination of MODIS-CERES satellite data and climate simulations, Atmos. Chem. Phys., 10, 9851–9861, doi:10.5194/acp-10-9851-2010, 2010.
Magarvey, R. H. and Geldart, J. W.: Drop Collisions under Conditions of Free Fall, J. Atmos. Sci., 19, 107–113, 1962.
McFarquhar, G. M.: The effect of raindrop clustering on collision-induced break-up of raindrops, Q. J. Roy. Meteor. Soc., 130, 2169–2190, doi:10.1256/Qj.03.98, 2004a.
McFarquhar, G. M.: A new representation of collision-induced breakup of raindrops and its implications for the shapes of raindrop size distributions, J. Atmos. Sci., 61, 777–794, 2004b.
McFarquhar, G. M. and List, R.: The Raindrop Mean Free-Path and Collision Rate Dependence on Rainrate for 3-Peak Equilibrium and Marshall-Palmer Distributions, J. Atmos. Sci., 48, 1999–2003, 1991a.
McFarquhar, G. M. and List, R.: The Evolution of 3-Peak Raindrop Size Distributions in One-Dimensional Shaft Models .2. Multiple Pulse Rain, J. Atmos. Sci., 48, 1587–1595, 1991b.
Mctaggart-Cowan, J. D. and List, R.: Acceleration System for Water Drops, J. Atmos. Sci., 32,

ACPD
11, 11739–11769, 2011

1395–1400, 1975.
Pruppacher, H. R. and Klett, J. D.: Microphysics of clouds and precipitation, D. Reidel, 1978.
Steiner, M. and Waldvogel, A.: Peaks in Raindrop Size Distributions, J. Atmos. Sci., 44, 3127–3133, 1987.
Stevens, B. and Feingold, G.: Untangling aerosol effects on clouds and precipitation in a buffered system, Nature, 461, 607–613, doi:10.1038/Nature08281, 2009.
Villermaux, E. and Bossa, B.: Single-drop fragmentation determines size distribution of raindrops, Nat. Phys., 5, 697–702, doi:10.1038/Nphys1340, 2009.
Warner, J.: Microstructure of Cumulus Cloud. I. General Features of Droplet Spectrum, J. Atmos. Sci., 26, 1049–1059, 1969.
Willis, P. T.: Functional Fits to Some Observed Drop Size Distributions and Parameterization of Rain, J. Atmos. Sci. , 41, 1648–1661, 1984.
Zawadzki, I. and Antonio, M. D.: Equilibrium Raindrop Size Distributions in Tropical Rain, J. Atmos. Sci., 45, 3452–3460, 1988.

ACPD
11, 11739–11769, 2011

Table 1. Drop breakup data, including initial and coalesced drop sizes. The large drop was approximately stationary during collision event; smaller drop velocity was determined from video footage.

	Breakup mode	small droplet vel ($m\,s^{-1}$)	small drop size (mm)	large drop size (mm)	Size ratio	Coalesced drop size (mm)	Theoretical terminal velocity difference ($m\,s^{-1}$)	Bin size (mm) & count					
								1	2	3	4	5	6
1	Bag	0.50	3	5	1.7	5	1.1	44	6	2	1	0	0
2		0.67	4	5	1.3	6	0.3	18	6	3	1	0	0
3		0.67	3	5	1.7	6	1.1	63	10	4	1	0	0
4		0.33	3	6	2.0	6	1.1	73	5	4	1	0	0
5		0.67	4	4	1.0	5	0.0	20	1	3	1	0	0
6		0.67	4	6	1.5	7	0.3	53	4	3	1	1	0
7		0.67	4	6	1.5	6	0.3	48	10	2	2	0	0
8		0.50	4	6	1.5	7	0.3	60	16	3	0	2	0
9		0.50	4	6	1.5	7	0.3	11	2	2	4	0	0
10		0.67	4	5	1.3	6	0.3	35	11	3	1	0	0
11		0.67	4	7	1.8	7	0.3	38	15	4	2	1	0
12		0.25	4	6	1.5	7	0.3	27	20	6	0	1	0
13		0.67	4	5	1.3	6	0.3	52	3	6	1	0	0
14	Sheet	0.40	4	6	1.5	7	0.3	8	4	5	2	1	0
15		0.67	4	6	1.5	7	0.3	2	4	2	1	0	1
16		0.50	4	5	1.3	6	0.3	6	6	3	0	1	0
17		0.33	4	6	1.5	6	0.3	34	9	5	1	0	0
18	Filament	0.67	4	6	1.5	8	0.3	7	1	1	0	2	0
19		0.67	4	8	2.0	9	0.3	1	3	3	0	1	1
20		0.67	3	5	1.7	6	1.1	3	0	1	0	1	1
21		0.67	4	6	1.5	7	0.3	2	2	1	0	1	1
22		0.50	4	5	1.3	6	0.3	0	2	1	1	1	0
23		0.50	4	6	1.5	7	0.3	8	4	1	1	2	0
24		0.67	4	6	1.5	6	0.3	10	6	4	0	1	0
25		0.40	4	6	1.5	7	0.3	2	3	0	1	0	1

	Mean												
	Bag	0.57	3.77	5.54	1.49	6.23		41.7	8.4	3.5	1.2	0.4	0.0
	Sheet	0.48	4.00	5.75	1.44	6.50		12.5	5.8	3.8	1.0	0.5	0.3
	Filament	0.59	3.88	6.00	1.55	7.00		4.1	2.6	1.5	0.4	1.1	0.5

ACPD
11, 11739–11769, 2011

The breakup of levitating water drops

C. Emersic and P. J. Connolly

Table 2. Factors to adjust the predicted percentage fraction of total resulting breakup fragments contributed by 4 and 6 mm drop-pair interactions based on the Low and List parameterisations. The adjusted range corresponds to initial cloud liquid water contents of 3 and 5 $kg\,kg^{-1}$. (See Appendix C for procedure to calculate k value and total estimated fragments.)

Breakup type	k value	Total estimated fragments	Observed average total fragments	Relative fractional difference	Adjusted maximum % fraction contribution of fragments
Filament	1.64×10^{-4}	2.46	10.15	4.13	2.1–4.5
Sheet	5.64×10^{-5}	5.66	24.75	4.37	2.2–4.8
Bag	2.60×10^{-4}	1.31	55.25	42.18	21.1–46.4

ACPD
11, 11739–11769, 2011

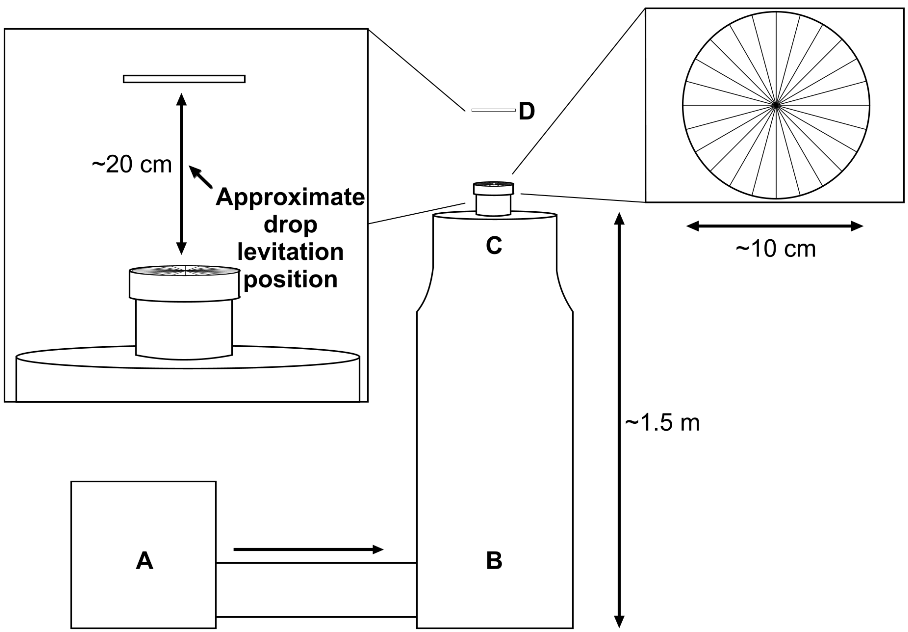

Fig. 1. Experimental setup; vertical wind tunnel: fan **(A)** blows air through into settling chamber **(B)** to minimise turbulence before exiting through top orifice **(C)**. Orifice is covered with a wire grate to produce a radial pressure profile which in conjunction with top plate **(D)** provides a back-pressure and creates a stagnation well in which drops can levitate.

ACPD
11, 11739–11769, 2011

C. Emersic and
P. J. Connolly

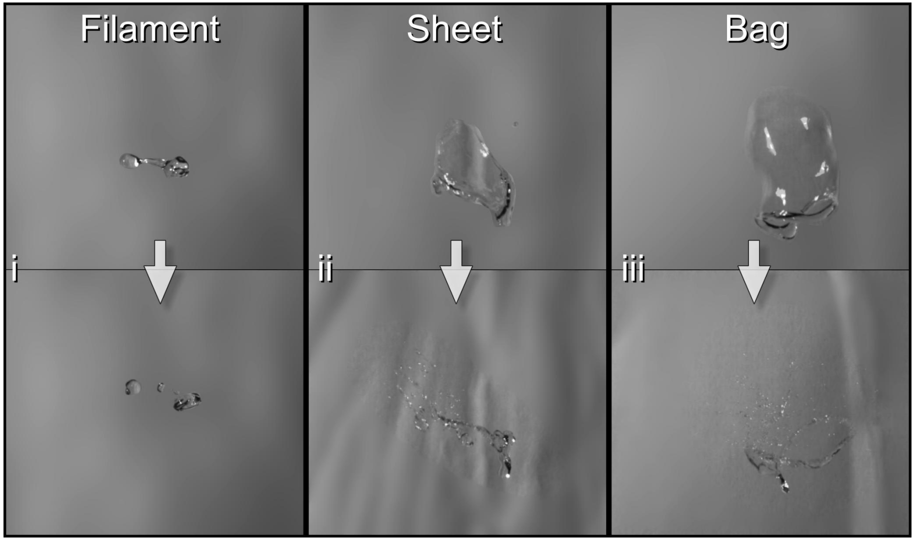

Fig. 2. Images of observed drop breakup types.

ACPD
11, 11739–11769, 2011

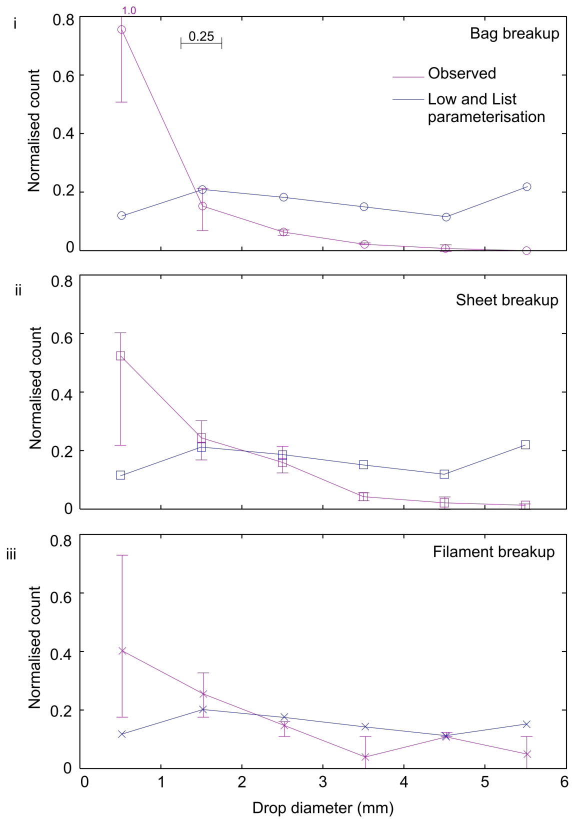

Fig. 3. Normalised histogram comparisons between observed drop breakup spectra and those predicted by the Low and List parameterisation for each breakup type. Bin values represent lower limit sizes; a drop diameter of "0" represents all particles between 0 and 1 mm, and so forth. Interquartile range is shown in observed results; horizontal bar in plot **(i)** represents what is deemed to be the maximum error in the drop size.

ACPD
11, 11739–11769, 2011

The breakup of levitating water drops

C. Emersic and P. J. Connolly

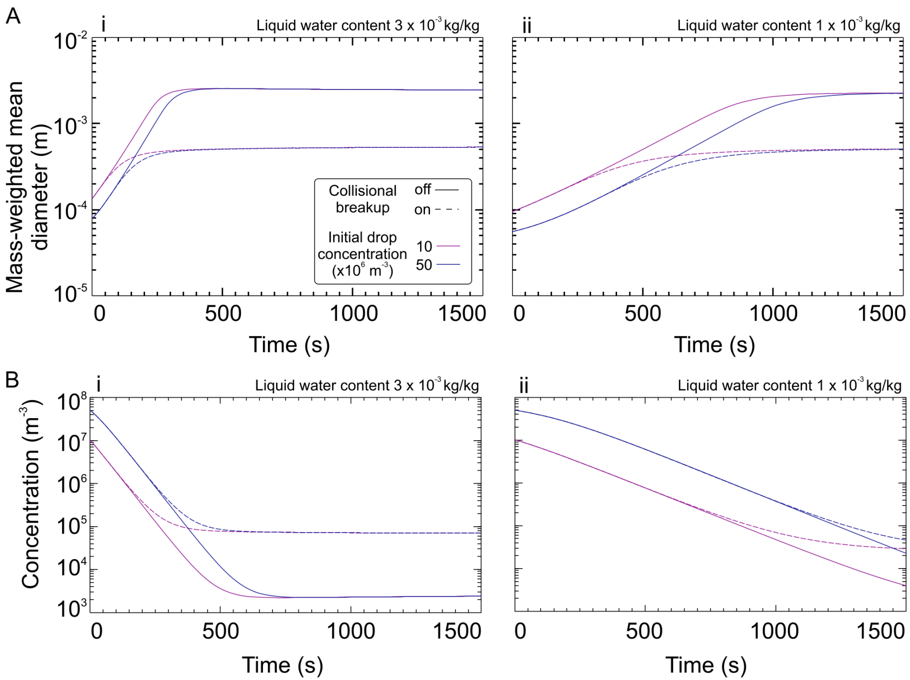

Fig. 4. Simulations of mass-weighted mean diameter and concentration changes during cloud evolution for 1500 s. Initial drop concentration and cloud liquid water content were varied for cases when collisional breakup was either active or inactive. Spontaneous breakup was active in all runs.

ACPD
11, 11739–11769, 2011

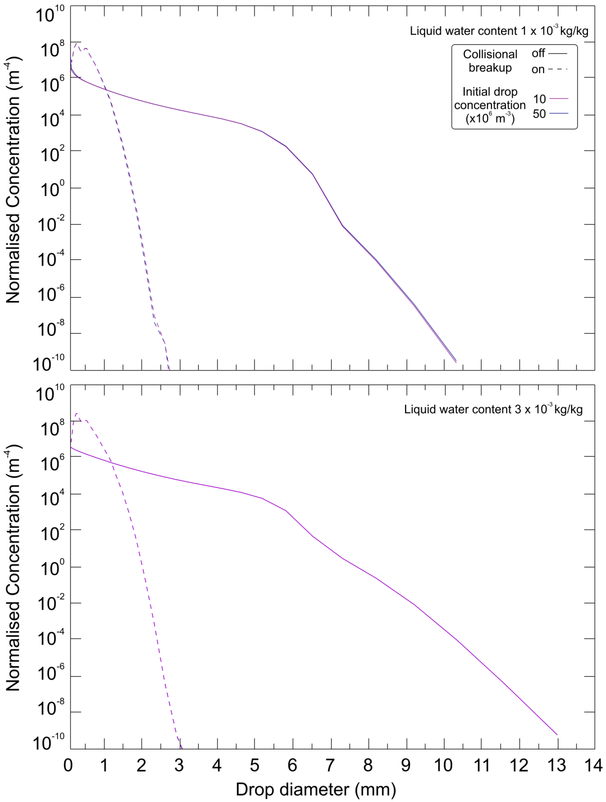

Fig. 5. Resulting simulation drop size distributions. Initial drop concentration and cloud liquid water content were varied for cases when collisional breakup was either active or inactive. Spontaneous drop breakup was active in all runs.

Discussion Paper | Discussion Paper | Discussion Paper | Discussion Paper |

ACPD
11, 11739–11769, 2011

The breakup of levitating water drops

C. Emersic and P. J. Connolly

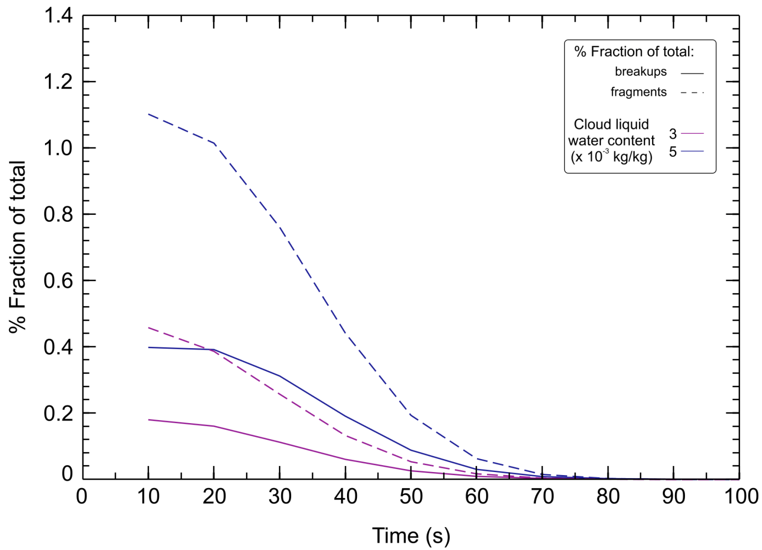

Fig. 6. The percentage fraction of total breakup events (solid lines) and percentage fraction of total resulting fragments (dashed lines) produced by a 4 and 6 mm drop-pair relative to all drop interactions. Cloud liquid water content was varied between large values of 3 kg kg^{-1} (pink) and 5 kg kg^{-1} (blue).

ACPD
11, 11739–11769, 2011

The breakup of levitating water drops

C. Emersic and P. J. Connolly